JOURNAL OF VIROLOGY, Nov. 2005, p. 13421–13433 Vol. 79, No. 21
0022-538X/05/$08.00+0 doi:10.1128/JVI.79.21.13421–13433.2005

VP24 of Marburg Virus Influences Formation of Infectious Particles

Sandra Bamberg, Larissa Kolesnikova, Peggy Möller, Hans-Dieter Klenk, and Stephan Becker*

Institut für Virologie der Philipps-Universität Marburg, Robert-Koch-Strasse 17, D-35037 Marburg, Germany

Received 14 March 2005/Accepted 6 July 2005

The highly pathogenic enveloped Marburg virus (MARV) is composed of seven structural proteins and the nonsegmented negative-sense viral RNA genome. Four proteins (NP, VP35, VP30, and L) make up the helical nucleocapsid, which is surrounded by a matrix that is composed of the viral proteins VP40 and VP24. VP40 is functionally homologous to the matrix proteins of other nonsegmented negative-strand RNA viruses. As yet, the function of VP24 remains elusive. In the present study we found that VP24 colocalized with inclusions in MARV-infected cells that contain preformed nucleocapsids and with nucleocapsids outside the inclusions. Coexpression studies revealed that VP24 is recruited into the inclusions by the presence of NP. Furthermore, VP24 displayed membrane-binding properties and was recruited into filamentous virus-like particles (VLPs) that are induced by VP40. The incorporation of VP24 altered neither the morphology of VLPs nor the budding efficiency of VLPs. When VP24 was silenced in MARV-infected cells by small interfering RNA technology, the release of viral particles was significantly reduced while viral transcription and replication were unimpaired. Our data support the idea that VP24 is essential for a process that takes place after replication and transcription and before budding of virus progeny. It is presumed that VP24 is necessary for the formation of transport-competent nucleocapsids and/or the interaction between the nucleocapsids and the budding sites at the plasma membrane.

Classified in the order *Mononegavirales*, the two *Filoviridae* family members, *Marburg virus* (MARV) and *Ebola virus* (EBOV), are both capable of causing hemorrhagic fevers with case fatality rates ranging from 30 to 90% (7). There are currently no approved vaccines or antiviral drugs available to prevent and/or treat filoviral diseases.

The enveloped MARV particles are composed of seven structural proteins and a nonsegmented negative-strand RNA genome of 19.1 kb (8). The viral envelope is spiked with homotrimers of the glycoprotein GP (9). The helical nucleocapsid is composed of four proteins: the nucleoprotein NP, the L protein, VP35, and VP30. NP, VP35, and L are essential for viral replication and transcription; the function of VP30, an NP-binding phosphoprotein, is still unclear (1, 21, 23, 24).

The matrix between the nucleocapsid and the viral envelope contains two proteins, VP24 and the highly abundant VP40. VP40 has been shown recently to display all features of a matrix protein, i.e., budding activity, membrane association, and nucleocapsid association (18, 20, 28). VP40 is transported to the plasma membrane using membranes of the late endosome and recruits the surface protein GP (which is transported via the exocytotic pathway) into VP40-containing multivesicular bodies. These, in turn, provide the platforms for the formation of the viral envelope (18, 19).

Virtually nothing is known regarding the structure and function of MARV VP24. VP24 is considered to be a second matrix protein, a unique feature in the order *Mononegavirales*. VP24 of EBOV was shown to strongly associate with lipid membranes and to induce its own release in the form of trypsin-resistant virus-like particles (VLPs) (15). Additionally, EBOV VP24 was assumed to play an important role in the formation of mature viral nucleocapsids, together with the polymerase cofactor VP35 (16). The essential role of VP24 for the formation of particles, however, is a matter of debate (31). Finally, VP24 is thought to represent an important pathogenicity factor of EBOV. In the course of adaptation of EBOV to guinea pigs, VP24 underwent significant structural changes that are believed to contribute to the high pathogenicity of the adapted virus (30).

Synthetically produced double-stranded RNA molecules (small interfering RNAs [siRNAs]) 19 to 21 nucleotides long have been shown to greatly decrease the intracellular amount of specifically targeted transcripts (6), and this approach has been used to impair viral replication (25). The siRNA technique has successfully been applied for the inhibition of poliovirus, influenza A virus, rotavirus, hepatitis B virus, respiratory syncytial virus, human immunodeficiency virus type 1, and recently for MARV (25, 11). Besides having a potential for antiviral therapy, siRNA technology may help us to better understand the basic mechanisms involved in virus replication. siRNA technology seems to be especially suitable to investigate the function of single viral proteins of negative-strand RNA viruses, since only the viral transcripts are accessible whereas the encapsidated genome is protected against the silencing by siRNA (3, 14).

In this study, we were able to show that VP24 interacts with lipid membranes and NP and is specifically recruited into VLPs formed by the major matrix protein VP40. Neither the budding efficiency of VP40-induced VLPs nor the morphology of released VLPs was influenced by the presence of VP24. Silencing of VP24 in MARV-infected cells, however, resulted in a significant reduction of released progeny virions, while the process of viral transcription and replication was unaltered.

* Corresponding author. Mailing address: Institut für Virologie der Philipps-Universität Marburg, Robert-Koch-Strasse 17, D-35037 Marburg, Germany. Phone: 49 6421 286 30 61. Fax: 49 6421 286 5482. E-mail: becker@staff.uni-marburg.de.

MATERIALS AND METHODS

Viruses. The Musoke strain of MARV, isolated in 1980 in Kenya, was propagated in C1008 cells and purified as described previously (13). Vero cells were infected under biosafety level 4 conditions with a multiplicity of infection of approximately 1 PFU per cell and fixed at 24 h postinfection. The recombinant vaccinia virus MVA-T7 was grown and titrated in chicken embryo fibroblasts as described by Sutter et al. (27).

Cells. Vero cells, human embryonic kidney (HEK293) cells, and HeLa cells were maintained in Dulbecco's modified Eagle medium (DMEM) supplemented with 10% fetal calf serum (FCS), L-glutamine, and penicillin-streptomycin solution. The cells were grown in an incubator at 37°C under 5% CO_2.

Antibodies. For indirect immunofluorescence (IF) and Western blot (WB) analysis, the following antibodies were used as primary antibodies: affinity-purified rabbit serum against MARV VP24 (dilution for IF, 1:2; dilution for WB, 1:10), rabbit serum against MARV GP (dilution for WB, 1:2,500), a mouse monoclonal antibody against MARV VP40 (kindly provided by the Centers for Disease Control and Prevention, Atlanta, GA) (dilution for IF, 1:100; dilution for WB, 1:3,000), a mouse monoclonal antibody against MARV NP (dilution for IF, 1:20), a guinea pig serum against VP30 (dilution for WB, 1:500), and a guinea pig serum against VP35 (dilution for WB, 1:5,000). Monoclonal antibodies against lysosome-associated membrane protein 1 (LAMP-1) and against annexin II were obtained from Transduction Laboratories (BD, Heidelberg, Germany) and used in dilutions according to the manufacturer's instructions. Secondary antibodies conjugated with fluorescein isothiocyanate (FITC) or rhodamine (Dianova) were used for immunofluorescence at a dilution of 1:400. Secondary antibodies conjugated with horseradish peroxidase (dilution for WB, 1:40,000) were obtained from Dianova (Hamburg, Germany).

Affinity purification of the MARV VP24 antibody from rabbit antiserum. To improve the specificity of the VP24 antibody and for reduction of nonspecific background activities, rabbit antiserum that was raised against bacterially expressed MARV VP24 was affinity purified. MARV antigen was separated by preparative sodium dodecyl sulfate-polyacrylamide gel electrophoresis (SDS-PAGE) and blotted onto polyvinylidene difluoride membrane. Viral proteins were visualized by Ponceau red staining, and the band corresponding to VP24 was cut out of the membrane. Unbound or loosely attached protein was removed by a 5-min treatment with 0.1 M glycine buffer (pH 2.5). The membrane was blocked at room temperature for 1 h with 3% bovine serum albumin (BSA) in Tris-buffered saline (TBS; 20 mM Tris-HCl, pH 7.4, 500 mM NaCl, 0.05% Tween-20 [vol/vol]). After being washed twice with TBS, the blot was incubated for 3 h at room temperature with rabbit antiserum against MARV VP24 diluted in TBS, followed by four washing steps with phosphate-buffered saline (PBS). For elution of the specifically bound VP24 antibody from the membrane, the blot was treated with 0.1 M glycine buffer (pH 2.5) for 10 min at room temperature, and the antibody-containing glycine buffer was transferred into a fresh cup and neutralized by the addition of 1 M Tris-HCl (pH 8). The elution step was repeated, and both eluates were joined and supplemented with BSA (final concentration of 1 mg/ml) and NaN_3 (final concentration of 5 mM). The resulting antibody was used for immunofluorescence and Western blot assays without further concentration.

DNA plasmids and molecular cloning. For generation of a plasmid encoding VP24, the region encompassing nucleotides 10182 to 11242 of the MARV genome (EMBL Nucleotide Sequence Database accession no. Z12132) was amplified by reverse transcriptase PCR using primers which facilitated cloning of the resulting PCR fragment into the BamHI restriction endonuclease site of the vector pTM1 (12). The resulting plasmid was designated pTM1-VP24. The vector pC-VP24 was generated by PCR amplifying the open reading frame of VP24 from the plasmid pTM1-VP24. The resulting fragment contained a SmaI site at the 5′ end and a NotI site at the 3′ end. This fragment was cloned into pCAGGS (pC) which was cut with the indicated restriction endonuclease enzymes. The forward primer contained the hemagglutinin sequence (encoding the peptide AYPYDVPDYA). Both primers contained a BamHI restriction site. The amplified fragment was cloned into the BamHI restriction site of pC.

The open reading frames of VP40 and GP (for reference, see EMBL Nucleotide Sequence Database accession no. Z12132) were subcloned from pTM1-VP40 (18) and pTM1-GP (26) into pC, using the restriction enzymes SmaI and NotI. All sequences were verified by automated sequencing. For expression of NP, the vector pTM1-NP was used (24).

siRNAs. siRNA oligonucleotides were purchased from QIAGEN (Hilden, Germany). The following sequences were used to target VP24: siRNA 1 (nucleotides 10465 to 10487), 5′-AACCGTTTTTGGCCCTGAGGATT-3′; and siRNA 2 (nucleotides 10819 to 10841), 5′-AACCTTGCTGTGGTGAGACAGTC-3′. A control siRNA (siRNA X) with no significant homologies with any known human or viral sequence was used as a nonspecific control (QIAGEN).

Transfection of HEK293 cells. At 24 h prior to transfection, HEK293 cells were trypsinized and transferred to Cellstar six-well plates (Greiner, Nürtingen, Germany). Cells were transfected with plasmids using Lipofectamine Plus reagent (Life technologies) according to the manufacturer's instructions. Transfected cells were incubated at 37°C for 24 h. Cotransfection of HEK293 cells with plasmids pC-VP40, pC-GP, and pC-VP24 was done with plasmid concentrations that resulted in a ratio of the expressed proteins that was similar to MARV-infected cells. The optimal proportion between pC-VP40 (5), pC-GP (1), and pC-VP24 (2.5) was 5:1:2.5. In all experiments, the total amount of transfected plasmids was held constant by adding empty vector (pCAGGS).

Subcellular fractionation and flotation assay. At 24 h posttransfection, HEK293 cells were washed three times with lysis buffer (10 mM Tris, pH 7.5, 0.25 M sucrose, 1 mM EDTA, 200 μM orthovanadate, 1 mM phenylmethylsulfonyl fluoride) at 4°C, scraped off the dish in a minimal volume of lysis buffer, and lysed by 10 strokes through a 20-gauge needle. Nuclei were pelleted for 5 min at 800 × *g* for 5 min at 4°C. Sucrose was added to the postnuclear supernatant to a final concentration of 63%. The sample was placed at the bottom of a centrifuge tube and overlaid with 45% and 10% sucrose. The discontinuous gradient was then centrifuged for 16 h at 35,000 rpm in a Beckman SW41 rotor. Fractions were collected from the top and supplemented with 4× sample buffer (100 mM Tris-HCl [pH 6.8], 4% SDS, 20% 2-mercaptoethanol, 20% glycerol, and 0.2% bromophenol blue). Equal amounts of each fraction were analyzed by SDS-PAGE and Western blotting. The effects of high salt or chelating agents on membrane association of VP24 were tested by treating the postnuclear supernatant before flotation analysis with either 2 M KCl or 50 mM EDTA for 1 h at 4°C.

Gel filtration. One six-well plate of HEK293 cells was transfected with 6 μg of pC-VP24 as described above. At 36 h posttransfection, cells were scraped off the dish and lysed in PBS containing Complete protease inhibitor (Roche, Mannheim, Germany) by three cycles of freeze-thawing in liquid nitrogen (5 min) and 37°C (5 min). Cell extracts were clarified twice at 13,000 rpm for 2 min and then filtered to remove cell debris. Total protein was separated by size on a Superdex-200 10/30 high-resolution fast-performance liquid chromatography column (Amersham Biosciences) by using an AKTA 10 purifier system (Amersham Biosciences). Eluted proteins were collected in 0.5-ml fractions, quantified, and analyzed by reducing SDS-PAGE and Western blot analysis.

Triton X-114 phase partitioning analysis. The phase partitioning analysis was done according to the method of Bordier (4). Briefly, VP24 and VP40 were expressed in HEK293 cells as described previously. At 24 h posttransfection, cells were scraped into ice-cold lysis buffer, disrupted with 10 strokes through a 20-gauge needle, and subjected to centrifugation for 5 min at 800 × *g* and 4°C to remove nuclei. The postnuclear supernatant was mixed with Triton X-114 (final concentration, 1% Triton X-114) in an ice water bath until the solution was clear. The sample was centrifuged at 14,000 × *g* for 15 min at 4°C to remove insoluble material. The supernatant was laid over a 300-μl sucrose cushion (6% [wt/vol] sucrose, 10 mM Tris, pH 7.8, 150 mM NaCl, 0.06% Triton X-114), warmed for 3 min at 30°C, and then centrifuged at 500 × *g* for 3 min at room temperature. The aqueous phase (top 200 μl) was collected, mixed with Triton X-114 again, laid over the same sucrose cushion used in the first extraction, and warmed and centrifuged as before. This resulted in a detergent phase combined from two extractions of the aqueous phase (~20 μl). The aqueous phase was mixed again with Triton X-114, placed over a new sucrose cushion, warmed, and centrifuged as before. The detergent phase (from the combined extractions) was collected and reextracted with 180 μl of buffer, placed over a new sucrose cushion, and processed as before; then the extraction was repeated once more. The aqueous and detergent phases were collected and adjusted to a final volume of 200 μl with lysis buffer, supplemented with 4× sample buffer, and analyzed by SDS-PAGE and Western blotting.

Purification of VLPs and proteinase K digestion. At 48 h posttransfection, the supernatant of HEK293 cells was saved and further treated as described below. To control the expression of the recombinant proteins in case they were not released into the medium, the cells were washed two times with PBS, resuspended in 400 μl of PBS, lysed by mixing with 200 μl of 4× sample buffer, and heated for 5 min to 96°C. Supernatants were centrifuged for 5 min at 1,500 × *g* to remove cell debris. Particulate material was then pelleted for 3 h at 35,000 rpm through a 20% sucrose cushion in a Beckman SW41 rotor. Pellets were resuspended in 60 μl of PBS and split into three aliquots of 20 μl. One sample was mixed with 4.6 μl of PBS, the second one was mixed with 2.2 μl of PBS and 2.4 μl of proteinase K in PBS (concentration, 1.5 μg/ml), and the third sample was mixed with 2.2 μl of PBS–1% Triton X-100 and 2.4 μl of proteinase K in PBS (concentration, 1.5 μg/ml). All three samples were incubated at 37°C for 1 h;

proteinase K was inactivated by the addition of phenylmethylsulfonyl fluoride, and 9 μl of 4× sample buffer was added. Samples were heated for 5 min to 96°C, separated by SDS-PAGE, and analyzed by Western blotting. Simultaneously, samples of the cell lysates (see above) were analyzed by SDS-PAGE and Western blotting.

Silencing of transiently expressed VP24. At 24 h before transfection, Vero cells were trypsinized and transferred to Cellstar 24-well plates (Greiner, Nürtingen, Germany) and grown to 70% confluence. A total of 250 ng of pC-VP24 with or without indicated amounts of siRNA was transfected into the cells using Lipofectamine 2000 according to manufacturer's instructions (Invitrogen, Karlsruhe, Germany). After 4 h, the transfection medium was removed from cells, and full medium was added. Fresh medium was reapplied after 24 h, and cells were harvested at 48 h posttransfection. To harvest cell lysates, monolayers were washed with PBS, trypsinized, and washed with DMEM, followed by centrifugation and a second washing step with PBS. After removal of PBS, 100 μl of cell lysis buffer (50 mM Tris-Cl, pH 7.5, 150 mM NaCl, 1.0% NP-40, 1.0 μg/ml), Complete protease inhibitor (Roche, Mannheim, Germany), and 2 U of DNase (Epicenter Technologies, Madison, Wis.) were added to cell pellets. Cell pellets were resuspended and incubated at 37°C for 10 min and finally supplemented with 4× sample buffer and boiled for 10 min. Protein concentrations were determined by performing SDS-PAGE, followed by Coomassie staining; the gel was analyzed using GelDoc 2000 (Bio-Rad, Richmond, USA) and the program TINA 2.09 (Raytest, Straubenhardt, Germany).

MARV infection and siRNA treatment. At 24 h before transfection, Vero cells were trypsinized and transferred to Cellstar six-well plates (Greiner, Nürtingen, Germany). Transfections, with the indicated amounts of siRNAs, were carried out as described by Bitko and Barik (3) with minor modifications. Cells were transfected with siRNAs using Lipofectamine 2000 in Opti-MEM I medium, and transfection medium was replaced at 4 h posttransfection with DMEM supplemented with 5% FCS. Cells were incubated for an additional 4 h and then infected with MARV at a multiplicity of infection of approximately 1 PFU per cell. At 1 h postinfection, cells were washed twice with DMEM, and a second siRNA transfection was performed. Four hours later, cells were washed and DMEM, supplemented with 10% FCS, was added. At 24 h postinfection, cells and supernatants were harvested. To harvest the supernatant, cell culture medium was centrifuged for 2 min at 8,000 × *g* to remove cellular debris. Supernatant was used for Western blot analysis, quantitative real-time reverse transcription-PCR (RT-PCR), and titration of released infectious viral particles.

For Western Blot analysis the supernatant was mixed with 4× sample buffer, boiled for 10 min, and subjected to SDS-PAGE. For real-time RT-PCR, viral RNA was purified from the supernatant using a QIAamp Viral RNA Mini Kit (QIAGEN, Hilden) according to manufacturer's instructions.

To harvest cells, monolayers were washed with PBS, trypsinized, and washed with DMEM, followed by centrifugation and a second washing step with PBS. After removal of PBS, 100 μl of cell lysis buffer was added to cell pellets. Cell pellets were resuspended and incubated at 37°C for 10 min and finally supplemented with 4× sample buffer and boiled for 10 min. Protein concentrations were quantified as described before.

Radioactive metabolic labeling and immunoprecipitation analysis. This experiment was performed essentially as described by Sänger et al. (26). Briefly, at 24 h after transfection, HUH-7 cells expressing Flag-tagged VP24 or NP and Flag-tagged VP24 were labeled for 30 min with 100 μCi of ^{35}S-Promix. Labeling medium was removed, and cells were chased in the presence of normal DMEM for 30 min. After being washed with ice-cold PBS, cells were lysed with TNES buffer (10 mM Tris-HCl, pH 7.5, 0.15 M NaCl, 2 mM EDTA, 1% NP-40, 0.5% SDS). Proteins (NP and VP24-Flag) were immunoprecipitated using antibodies specific for the Flag tag and NP. The precipitated samples were subjected to SDS-PAGE. The radioactive signals were visualized by exposing dried gels to a BioImager plate and were scanned by using a bioimaging analyzer (BAS-1000; Fuji).

Western blot analysis. After electrophoretic transfer of proteins onto polyvinylidene difluoride membranes, the membranes were blocked at 4°C overnight with 10% milk powder in PBS. The blots were incubated for 1 h with the respective primary antibody diluted in PBS supplemented with 1% milk powder and 0.1% Tween 20, followed by incubation with a secondary antibody coupled with horseradish peroxidase (Dianova). Bound antibodies were visualized using the SuperSignal chemoluminescence substrate as described by the supplier (Pierce, Rockford, Ill.).

Real-time RT-PCR. To compare the amount of viral RNA in the supernatant of MARV-infected Vero cells with and without siRNA treatment, real-time RT-PCR using the SuperScript One-Step RT-PCR with Platinum *Taq* Kit (Invitrogen) according to manufacturer's instruction was performed.

The primers used for the PCR were 5′-CATGACTTGATTCAAAGAATA TAC-3′ (forward) and 5′-CCTCATATCTGTTATCATCTA-3′ (reverse). The PCR was set up according to the supplier's protocol. The PCR cycle parameters were 95°C for 5 s, 60°C for 10 s, and 72°C for 20 s. Quantification and digitalization were done with a LightCycler (Roche).

Virus titration. The supernatant of MARV-infected cells was harvested at 24 h postinfection and sequentially diluted, and a 50% tissue culture infective dose test was performed on Vero cells as described by Traggiai et al. (29). The cytopathic effect of MARV was determined at 8 days postinfection.

Immunofluorescence analysis. Subconfluent HeLa cells grown on glass coverslips were infected at a multiplicity of infection of 3 to 5 PFU of MVA-T7 per cell. At 1 h postinfection, cells were transfected with 1 μg of pTM1-VP24 (encoding VP24), 1 μg of pTM1-NP (encoding the nucleocapsid protein NP), or both plasmids by using Lipofectin (Invitrogen, Karlsruhe, Germany) as described previously (10). The overall amount of transfected plasmids was held constant by adding empty vector (pTM1). The cells were washed with PBS at 12 h posttransfection and fixed with 4% paraformaldehyde for 15 min. Subconfluent Vero cells on glass coverslips were infected with MARV at a multiplicity of infection of approximately 1 PFU per cell. At 1 h postinfection, cells were washed with DMEM supplemented with 10% FCS. At 24 h postinfection, cells were washed with PBS and fixed with 4% paraformaldehyde overnight.

For immunofluorescence staining, cells were rinsed two times with PBS and incubated with 0.1 M glycine in PBS for 5 min at room temperature. Thereafter, cells were washed once with PBS and permeabilized with PBS containing 0.1% Triton X-100. After being washed with PBS, cells were incubated in blocking solution (2% BSA, 0.2% Tween 20, 5% glycerol in PBS) and incubated first with the appropriate primary antibodies and then with secondary antibodies as indicated in the figure legends. Microscopic analysis was performed using an Axiomat fluorescence microscope (Zeiss).

Electron microscopy. Electron microscopic and immunoelectron microscopic analyses were performed as previously described (18).

RESULTS

Recombinant VP24 is associated with intracellular membranes. It has been presumed that VP24 represents a minor matrix protein of MARV. We therefore addressed the question of whether MARV VP24 is able to interact with lipid membranes. VP24 was expressed in HEK293 cells that were lysed at 24 h posttransfection. The lysates were subjected to flotation analysis (2) (Fig. 1A). Under the chosen experimental conditions, a small amount of VP24 was detected at the 45 to 10% sucrose interface comigrating with LAMP-1, which was used as a marker for membrane-containing fractions (fractions 2 to 4). The majority of VP24 was found in the loading zone together with annexin II, which served as a soluble control protein (fractions 10 and 11). Next, we investigated whether the presence of the integral viral surface protein GP or the peripherally membrane-associated matrix protein VP40 could recruit VP24 to cellular membranes. These analyses showed that neither VP40 nor GP was able to alter the amount of membrane-bound VP24 (data not shown). Additional flotation experiments were carried out with VP24-expressing cell lysates that were treated with high salt (2 M KCl) or EDTA before flotation analysis. We found that none of these treatments altered the membrane association of VP24 (data not shown).

Oligomerization state of VP24. The function of viral matrix proteins in assembly and budding is dependent upon their ability to oligomerize. We therefore determined whether VP24 could homooligomerize in mammalian cells. HEK293 cells were transfected with pC-VP24; cells were harvested after an incubation time of 36 h, and the cell lysate was analyzed by gel filtration and Western blot analyses of the resulting fractions. We detected VP24 eluting from the column in three distinct peaks (Fig. 1B). The first peak of VP24 protein was detected in

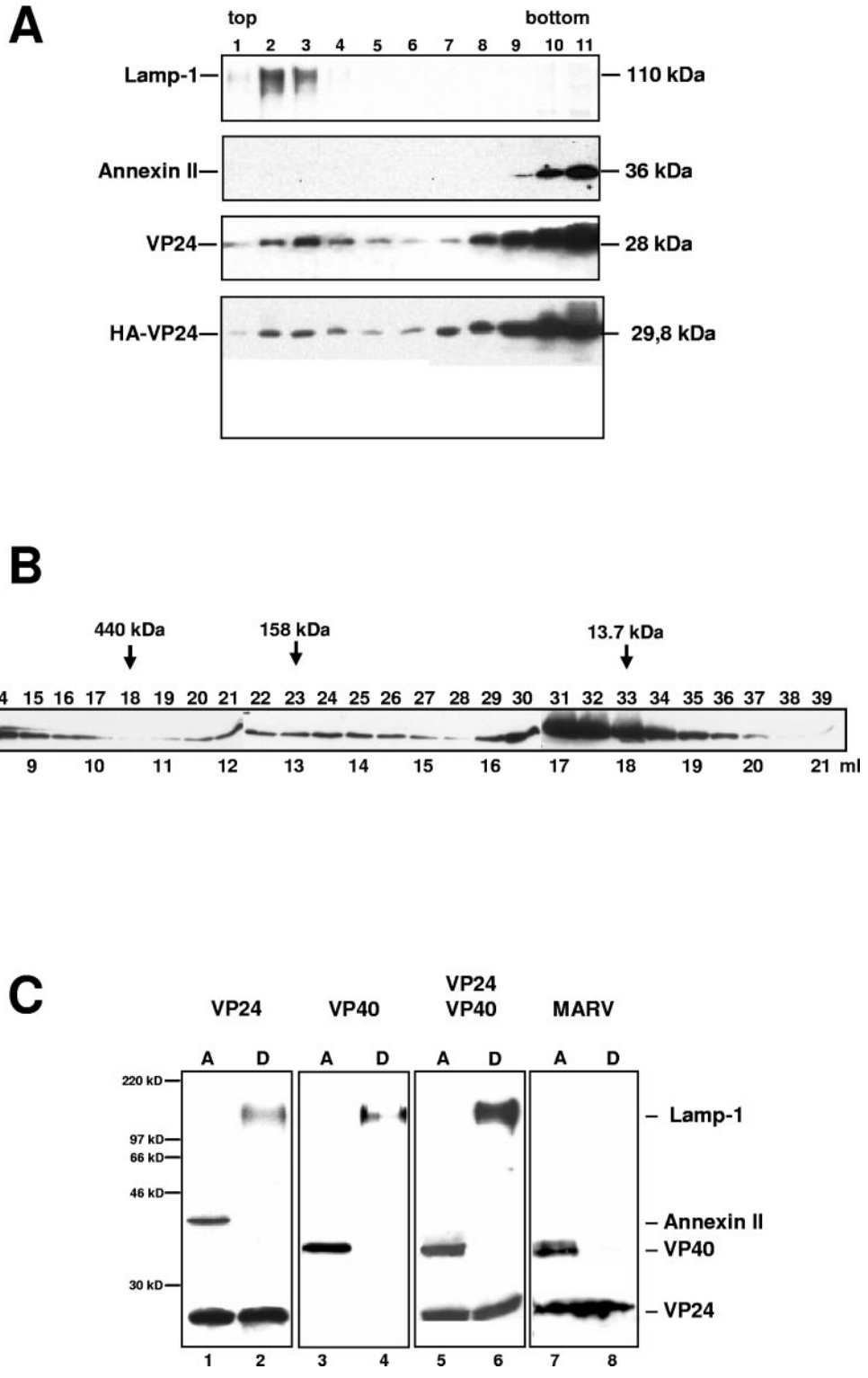

FIG. 1. Membrane association of VP24. (A) HEK293 cells were transfected with pC-VP24 and harvested at 24 h posttransfection, and cell lysates were subjected to flotation analysis via discontinuous sucrose gradient. The gradient was centrifuged to equilibrium at 35,000 rpm overnight in a Beckman SW41 rotor. Fractions were collected from the top, and samples were analyzed by SDS-PAGE and Western blotting. Membranes were stained with anti-LAMP-1 (monoclonal), anti-annexin II (monoclonal), and anti-VP24 (rabbit), respectively. Top of the gradient, fraction 1; bottom of the gradient, fraction 11. (B) Gel filtration and Western blot analyses of VP24. HEK293 cells were transfected with pC-VP24, and cell extracts were harvested at 36 h posttransfection. Clarified and filtered cell lysate was separated by size on a Superdex-200 10/30 high-resolution fast-performance liquid chromatography column. Molecular mass standards were also separated on the same column. A Western blot analysis of fractions representing elution volumes of 8.0 to 21.0 ml is shown. One peak of VP24 eluted within the 13.5-ml volume, which corresponds to a protein of approximately 120 kDa (tetramer). The majority of VP24 appeared at elution volume of 17.5 ml and corresponded to the monomeric

early fractions in the 8-ml elution volume corresponding to large protein aggregates. The second peak around fraction 24 corresponded to the elution volume of 13.5 ml and to proteins with molecular masses of approximately 115 to 120 kDa as determined by the elution profile of the molecular mass standards. This size corresponds to a tetrameric form of VP24 (~112 kDa). The majority of VP24 was found in fractions 31 and 32 (elution volume of 17 to 17.5 ml) in a monomeric form (~28 kDa), as indicated by the elution profile of the molecular mass standard.

These results suggested that VP24 can oligomerize and that VP24 oligomers preferentially represent tetramers. The presence of additional oligomeric forms of VP24 (e.g., dimers, trimers, and pentamers) cannot be ruled out completely. The ability of VP24 to homooligomerize is consistent with a potential role in virion assembly.

VP24 partitions with Triton X-114. The membrane association of VP24 was further characterized using Triton X-114 phase partitioning analysis, which allows a determination of whether proteins are integral membrane proteins or peripherally associated to lipid membranes. The postnuclear supernatants of HEK293 cells expressing VP24, VP40, or both proteins were incubated with Triton X-114 and centrifuged to separate the aqueous (soluble and peripheral membrane proteins) and detergent (integral membrane proteins) phases. VP24 was detected in equal amounts in the detergent phase and in the aqueous phase (Fig. 1C, lanes 1 and 2). The integral membrane protein LAMP-1 was only found in the detergent phase of the extraction (lanes 1 and 2), whereas the predominantly soluble annexin II was found in the aqueous phase (lanes 1 and 2). VP40, which represents a peripheral membrane protein, was exclusively detected in the aqueous phase (Fig. 1C, lanes 3 and 4) (20). Triton X-114 solubility of VP24 and VP40 was not changed upon coexpression of both proteins (Fig. 1C, lanes 5 and 6). Triton X-114 phase partitioning analysis of virion-associated VP24 also showed that the protein was equally partitioned into the aqueous and detergent phase (Fig. 1C, lanes 7 and 8). Taken together, the results show that either the hydrophobic VP24 interacts weakly with cellular membranes or only a fraction of VP24 is able to bind to lipid membranes. Gel filtration experiments revealed a tendency of VP24 to oligomerize. Moreover, VP24 partly displays features of an integral membrane protein. The presence of neither VP40 nor GP had impact on membrane binding of VP24. It remains unclear whether homooligomerization of VP24 might support the ability of the protein to interact with cellular membranes.

VP24 is associated with nucleocapsids and cellular membranes in MARV-infected cells. The intracellular localization of VP24 was analyzed in MARV-infected Vero cells using indirect immunofluorescence and immunoelectron microscopic analyses. At 24 h postinfection, VP24 was present in large aggregates in the perinuclear region and diffusely distributed in the cytoplasm (Fig. 2A, frame set 1, arrows). Simultaneous staining with anti-NP antibodies showed that the VP24 positive perinuclear aggregates represented viral inclusions which are sites of formation and accumulation of nucleocapsids (Fig. 2A, frame sets 2 and 3, arrows) (21). This result was confirmed by immunoelectron microscopy investigations. VP24 was detected in the electron-dense viral inclusions (Fig. 2B, arrowheads) and was colocalized with single nucleocapsids in the cytoplasm and beneath the plasma membrane (Fig. 2C, arrows in left and right frames, respectively).

We further investigated cytoplasmic distribution of VP24 and focused on colocalization with VP40. While the majority of VP40 in MARV-infected cells was located in multivesicular bodies that belong to the late endosomal compartment, these structures were practically free of VP24. (Fig. 2D, frame I; arrows indicate VP40) (20). VP24 was associated with other intracellular membranes of as yet unknown origin which did not contain VP40 (Fig. 2D, frames II and III; arrows indicate VP40 and arrowheads indicate VP24). At the plasma membrane, VP24 was found to be localized in the same membrane protrusions as VP40 (Fig. 2D, frame IV). These plasma membrane protrusions did not show the presence of nucleocapsids. Finally, colocalization of VP24 and VP40 was also detected in released virions (Fig. 2D, frame V). Taken together, these results show that intracellular VP24 colocalized with (i) NP-induced inclusions that contain nucleocapsid structures and (ii) single nucleocapsids and that VP24 was found in the same plasma membrane area as VP40. These results indicated that VP24 was transported to the plasma membrane in two ways. On the one hand, VP24 was cotransported with nucleocapsids; on the other hand, VP24 was transported independently of nucleocapsids and mixed at or near the plasma membrane with VP40 before particles were released.

Recruitment of VP24 to viral inclusions and nucleocapsids is mediated by NP. It was of interest to find out which of the viral nucleocapsid proteins was responsible for recruiting VP24 into the inclusions. Since NP is the main nucleocapsid component, we investigated whether VP24 could interact with NP. To this end, intracellular localization of recombinant VP24 was investigated upon single expression and coexpression with NP in HeLa cells using the MVA-T7 system. Singly expressed VP24 was detected at 16 h posttransfection in small aggregates in the perinuclear region morphologically distinguishable from the inclusions in MARV-infected cells (Fig. 3A, frame 1). Additionally, a faint signal of VP24 was detected at the plasma membrane. Single expression of NP resulted in the formation of typical inclusions in the perinuclear region (Fig. 3A, frame 2) (1, 21). Coexpression of both proteins led to a clear relocalization of VP24 from the smaller aggregates into the large inclusions formed by NP (Fig. 3A, frames 3 to 5). These results demonstrated that VP24 is recruited to the viral nucleocapsids by the presence of NP and explain the nucleocapsid association

form of VP24 (~28 kDa). (C) Triton X-114 phase partitioning analysis of VP24. HEK293 cells were transfected with pC-VP24, pC-VP40, or both plasmids and cells were harvested at 24 h posttransfection. MARV particles from the supernatant of infected Vero cells were purified over a sucrose cushion prior to phase partitioning. Postnuclear supernatants of HEK293 cells and purified MARV particles were partitioned into aqueous (A) and detergent (D) phases as described in Materials and Methods and analyzed by SDS-PAGE and Western blotting. Blots were cut horizontally to get pieces corresponding to the targeted proteins, and the pieces were stained separately using anti-LAMP-1 (mouse monoclonal), anti-annexin II (mouse monoclonal), anti-VP24 (rabbit), and anti-VP40 (rabbit) antibodies, respectively.

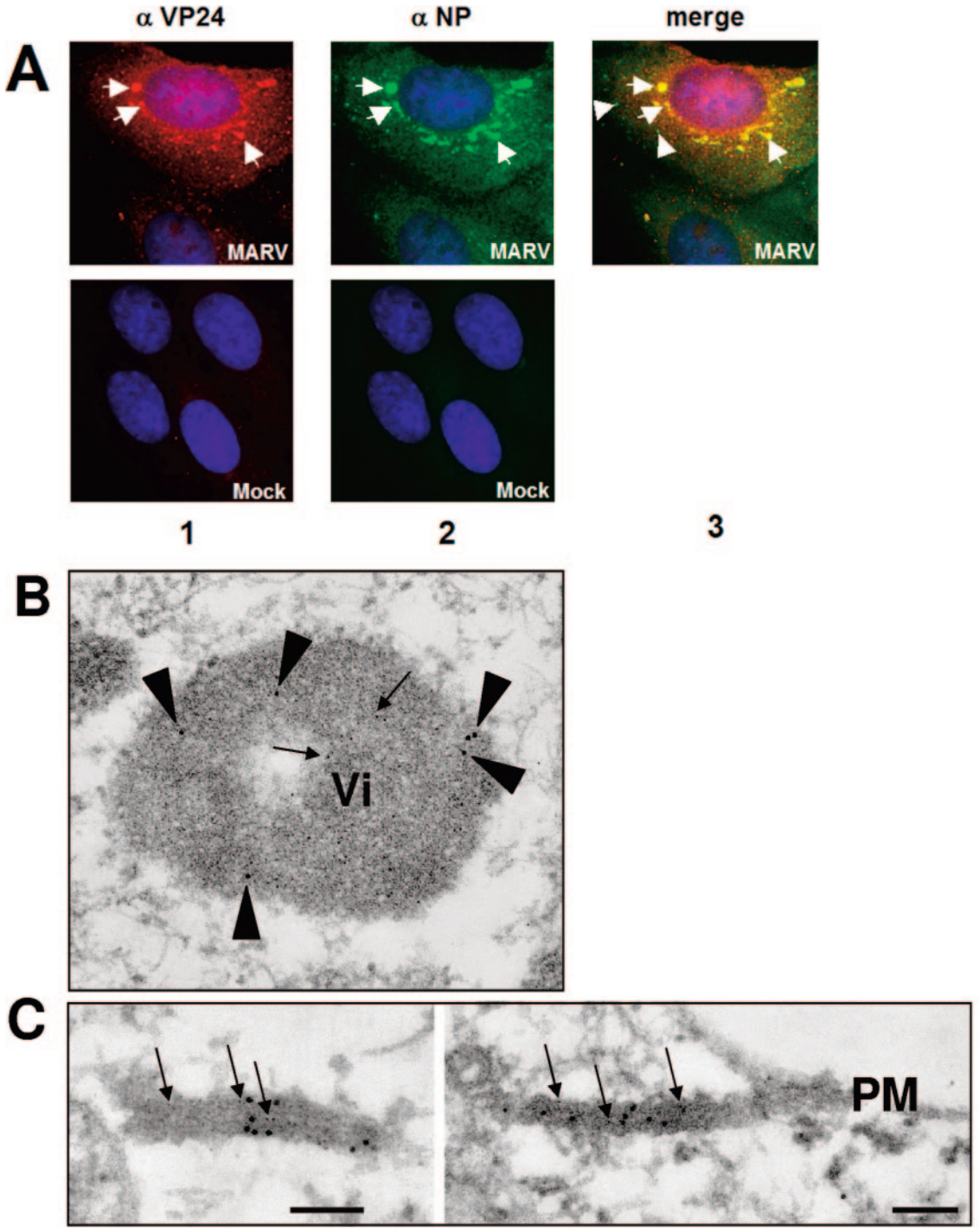

FIG. 2. Immunofluorescence and immunoelectron microscopic analysis of VP24 in MARV-infected cells. (A) Distribution of VP24 in MARV-infected cells. Vero cells were infected with MARV and fixed 24 h postinfection. For immunofluorescence analysis, a rabbit anti-VP24 antibody and a monoclonal anti-NP antibody were used as primary antibodies. Donkey anti-rabbit immunoglobulin G conjugated with rhodamine and goat anti-mouse antibody conjugated with FITC were used as secondary antibodies. Arrows, colocalization of VP24 with NP; arrowheads, singly located NP. (B to D) Immunoelectron microscopic analysis of the ultrathin sections of MARV-infected Vero cells. Vero cells were fixed at 48 h postinfection and embedded in LR Gold, and ultrathin sections were subjected to immunoelectron microscopy. (B and C) Samples were stained using rabbit anti-VP24 and mouse anti-NP primary antibodies. Secondary antibodies were used as described for panel D. Arrows, NP; arrowheads, VP24. Bar, 100 nm. (B) Viral inclusion (Vi). (C) Single nucleocapsid in the cytoplasm (left) and single nucleocapsid near the plasma membrane (PM, right). (D) Samples were stained using rabbit anti-VP24 and mouse anti-VP40 primary antibodies. As secondary antibodies goat anti-rabbit antibody conjugated with 12-nm gold and goat anti-mouse antibody conjugated with 6-nm gold were used. Arrows, VP40; arrowheads, VP24. Bar, 200 nm. Shown are a multivesicular body containing VP40 (I), cytoplasm containing separately located VP40 and VP24 (II), cellular protrusion with VP40 and VP24 below the plasma membrane (III), cellular protrusions containing both VP24 and VP40 at the plasma membrane (IV), and released viral particles containing VP40 and VP24 (V).

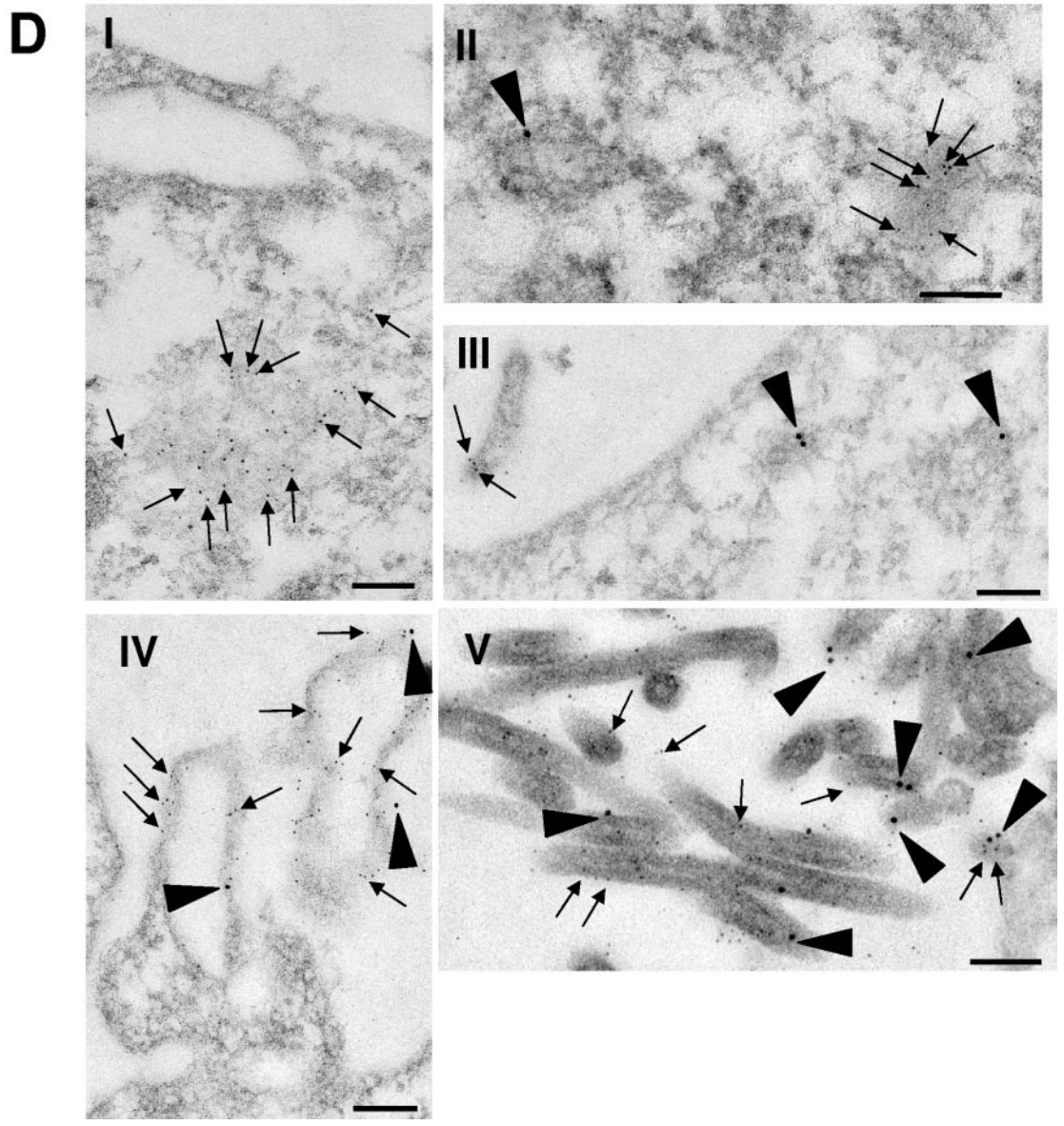

FIG. 2—*Continued.*

of VP24. By using coimmunoprecipitation analysis, we found that VP24 did not coimmunoprecipitate NP and vice versa (Fig. 3B, lanes 3 and 7). This result suggested that the interaction between NP and VP24 is either very weak or transient or that VP24 interacts with an oligomeric form of NP that was not targeted in the used approach.

VP24 is recruited into the VP40-induced VLPs. We further investigated (i) whether VP24 is able to form VLPs and (ii) whether VLP formation by VP40 is influenced by the presence of VP24 and/or GP. VP24, VP40, and GP were expressed alone or in combination in HEK293 cells, and the supernatants were harvested at 48 h posttransfection. Released VLPs were purified from the supernatant and analyzed by Western blotting. Lysates of transfected cells served as expression controls (Fig. 4A, left). Upon single expression, no VP24 could be detected in the supernatant (Fig. 4A, right, lane 1). Coexpression of VP24 and VP40 resulted in the release of VP24 into the supernatant (Fig. 4A, right, lane 4). The amount of released VP40 was not altered by the presence of VP24 (Fig. 4A, right, lanes 2 and 4). Coexpression of GP and VP24 did not lead to the recruitment of VP24 into vesicles that are induced by the expression of GP (Fig. 4A, right, lanes 3 and 5) (19, 26). As described previously, coexpression of VP40 and GP resulted in an enhanced release of both proteins (Fig. 4A, lanes 2, 3, and 7) (18). When VP24, VP40, and GP were coexpressed, VP24 was recruited into the VLPs composed of VP40 and GP. While the amount of released VP40 was not changed upon triple expression, we observed frequently that the amount of GP in the supernatant was slightly diminished in comparison with coexpression of VP40 and GP (Fig. 4A, right, lanes 6 and 7).

We then investigated the intraparticle localization of VP24 in VLPs. VLPs were purified from cells expressing VP40 and

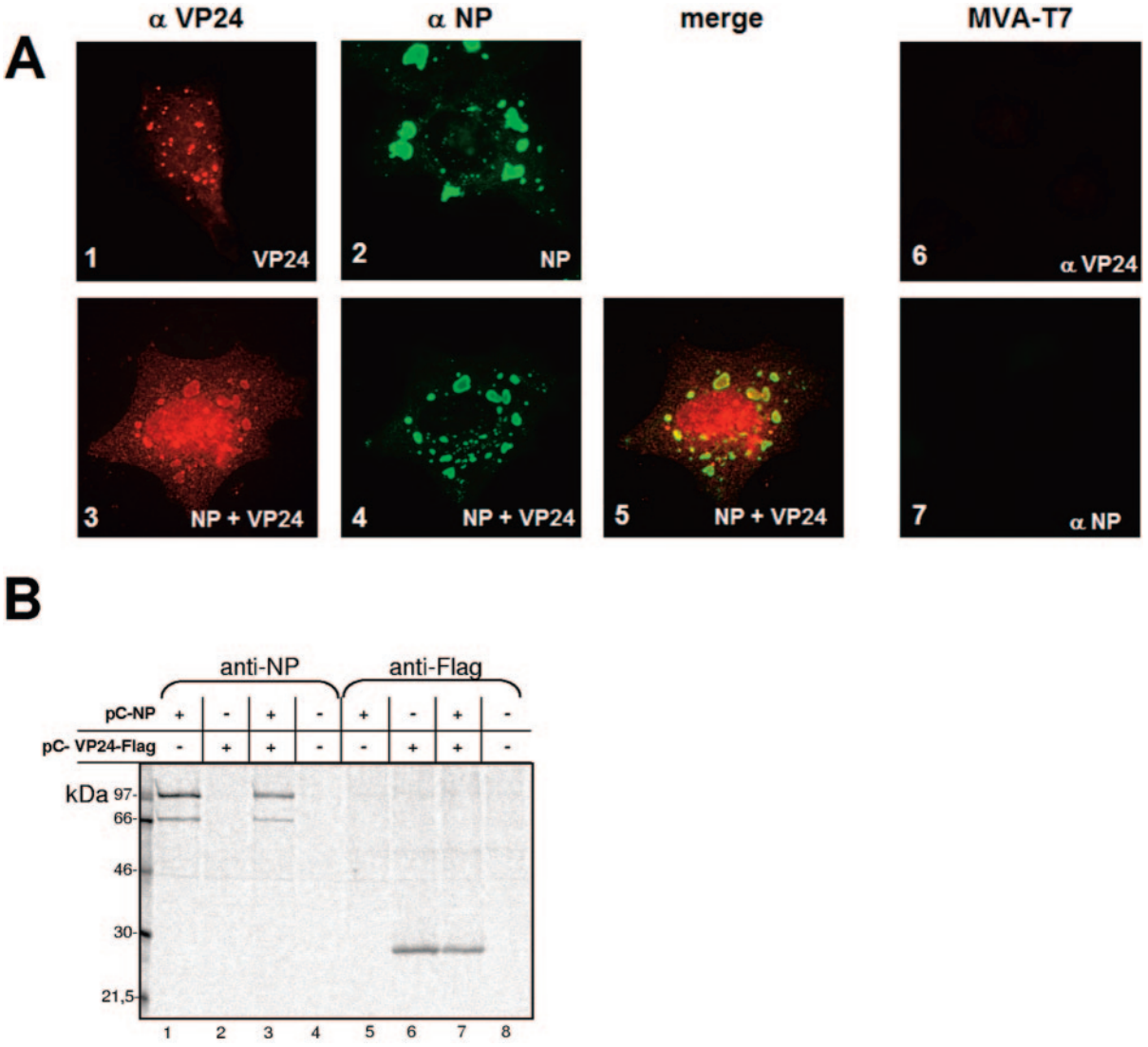

FIG. 3. Influence of NP on the intracellular distribution of recombinant VP24. (A) Localization of VP24 upon single expression and upon coexpression with NP. HeLa cells were infected with MVA-T7 and transfected with pT-VP24, pT-NP, or both plasmids. At 16 h posttransfection, cells were fixed and immunostained with a rabbit anti-VP24 antibody, a secondary donkey anti-rabbit immunoglobulin G conjugated with rhodamine and with an anti-NP monoclonal antibody, and a secondary goat anti-mouse antibody conjugated with FITC. (B) Coimmunoprecipitation of NP and VP24. HUH-7 cells expressing either VP24, NP, or VP24 and NP were metabolically labeled with ^{35}S-Promix. Cells were lysed at 25 h posttransfection. Cell lysates were immunoprecipitated with either NP or anti-Flag.

VP24 and subjected to proteinase K treatment. It turned out that the released VP24 was proteinase K resistant (Fig. 4B, lane 2). In the presence of Triton X-100, which destroys lipid membranes, VP24 and VP40 became proteinase K sensitive (lane 3). Analysis of the VLPs by immunoelectron microscopy confirmed the presence of VP24 in the filamentous VP40-specific VLPs (Fig. 4C, arrows). Since protease digestion revealed that VP24 was located beneath the lipid membrane, it was not surprising that antibodies only had access to VP24 (arrow) at places where the membrane integrity of VLPs was obviously impaired. Taken together, these experiments revealed that VP24 is not able to form VLPs alone but is incorporated into VP40-induced VLPs even in the absence of other viral proteins. The presence of VP24 did not alter the efficiency of VLP release. The incorporation was specific for VP40-induced VLPs, since VP24 was not recruited into GP-induced vesicles.

Silencing of VP24 in transient expression. To analyze whether VP24 is essential for the MARV replication cycle, we used RNA interference technology to silence VP24 transcripts. Selection of siRNA sequences was made following the "Tuschl rules" (http://www.rockefeller.edu/labheads/tuschl/sirna.html). First, the two chosen VP24-specific siRNA molecules siRNA-VP24 1 and 2 were checked for functionality in Vero cells transiently expressing VP24. As a negative control siRNA, we used a commercial siRNA with no significant homology to cellular or MARV genome targets (siRNA X). Plasmid pC-VP24 was transfected together with different amounts of siRNAs into Vero cells. At 48 h posttransfection, cell lysates were collected, and Western blotting was performed to detect

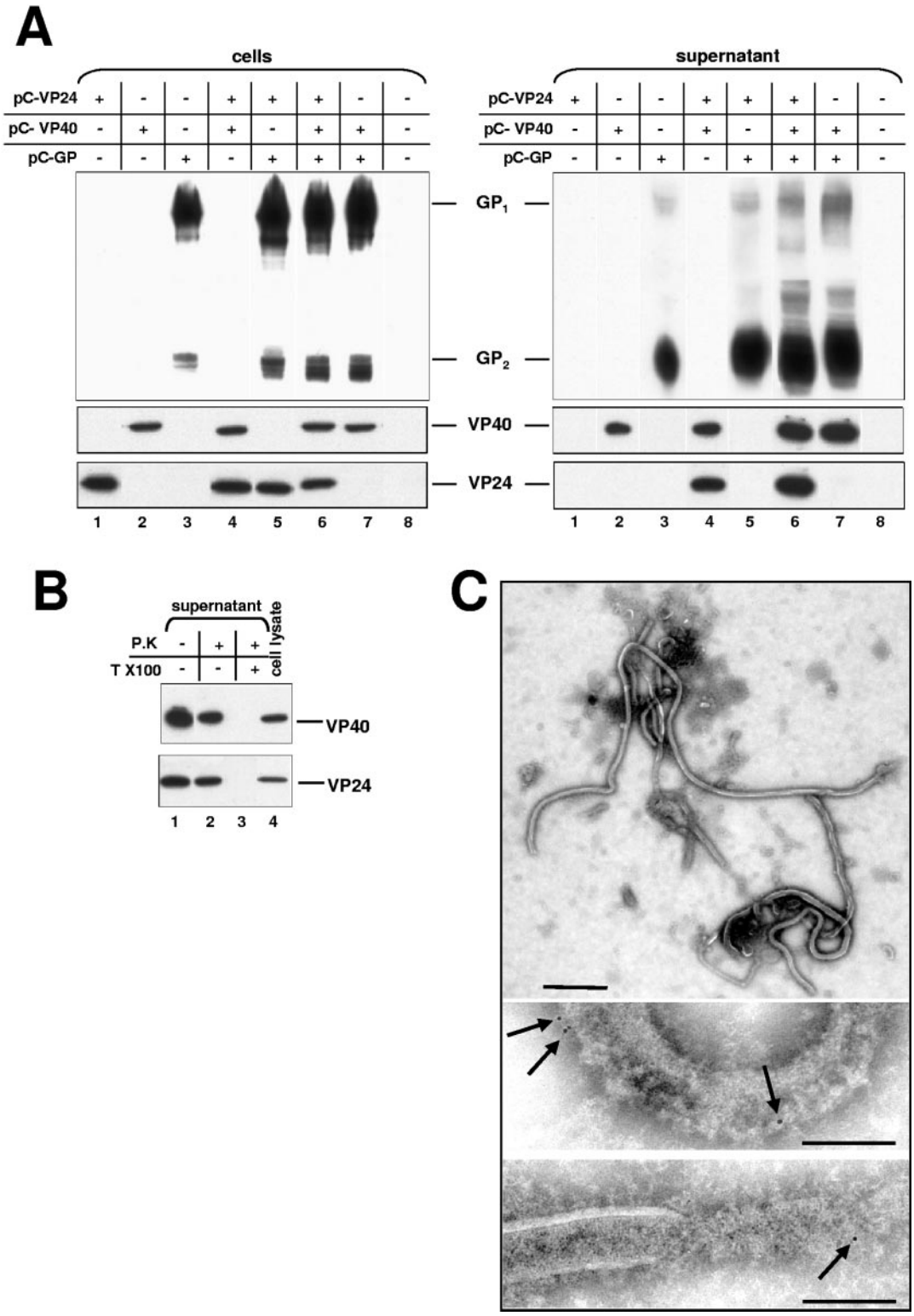

FIG. 4. Release of VP24 associated with VLPs. (A to C) HEK293 cells were transfected with the plasmids encoding the proteins indicated above the blots. At 48 h posttransfection, the cells and particulate material of cellular supernatant were harvested as described in Materials and Methods. (A) Cell lysates and particulate material in supernatant of cells transfected with various combinations of VP24, VP40, and GP. (B) Proteinase K digestion of VLPs purified from the supernatant of cells coexpressing VP24 and VP40. Lane 4, cell lysate. (C) Electron microscopy analysis of VLPs formed by coexpression of VP24 and VP40. The top frame shows VLPs at low magnification. Bar, 1,000 nm. The two lower frames show immunostaining of purified VLPs with rabbit anti-VP24 and goat anti-rabbit antibodies conjugated with 6-nm gold. The antibodies recognized VP24 (arrows) only at places where the membrane was partly destroyed. Bar, 100 nm.

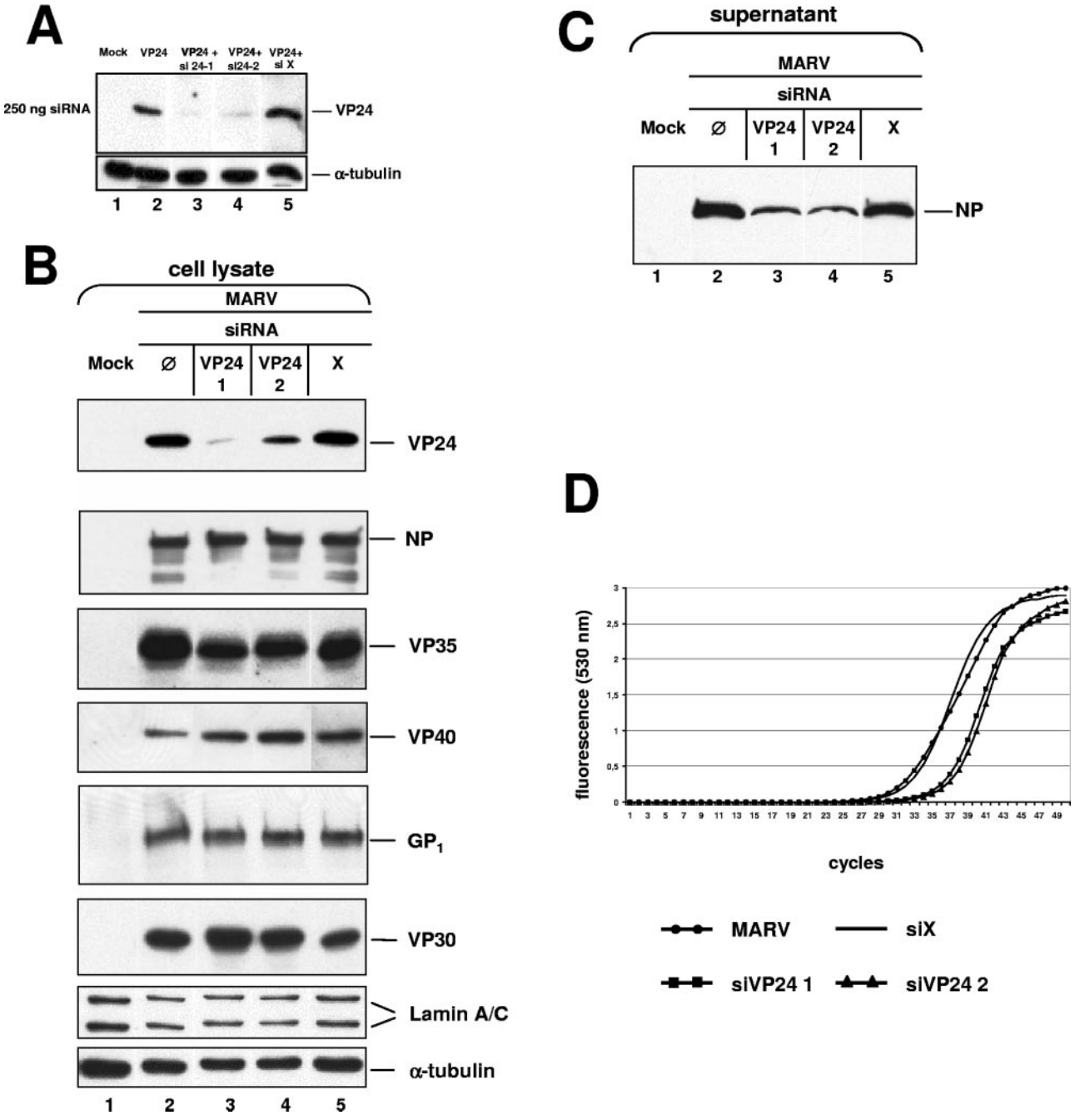

FIG. 5. RNA interference treatment of VP24-transfected and MARV-infected Vero cells. (A) Silencing of transiently expressed VP24. Vero cells were cotransfected with 250 ng of pC-VP24 and 250 ng (30 nM) of VP24-specific siRNA 1 or 2 and control siRNA X. At 48 h posttransfection, lysates were collected, and Western blotting was performed to detect VP24 and the cellular protein α-tubulin. Equal amounts of protein were loaded onto gels for SDS-PAGE. Lane 1, 250 ng of empty plasmid; lane 2, 250 ng of pC-VP24; lane 3, pC-VP24 plus 250 ng of siRNA VP24 1; lane 4, pC-VP24 plus 250 ng of siRNA VP24 2; lane 5, pC-VP24 plus 250 ng of control siRNA X. (B) Silencing of VP24 in MARV infection. Vero cells were transfected with 44 nM (1,543 ng) specific siRNAs or control siRNA X. At 8 h posttransfection, cells were infected with MARV followed by a second siRNA transfection. At 24 h postinfection, lysates were collected and protein amounts were determined. Equal amounts of protein were loaded, and Western blotting was performed to detect VP24, NP, VP35, VP40, GP, VP30, α-tubulin, and lamin A/C. (C) Release of progeny virus from cells after siRNA treatment. Vero cells were transfected and infected as described for panel B. At 24 h postinfection, supernatants were harvested and analyzed by Western blotting using an anti-NP antibody. (D) Real-time RT-PCR of genomic viral RNA released into the supernatant. Vero cells were transfected and infected as described for panel B. At 24 h postinfection, supernatants were harvested, and viral RNA was purified via a QIAamp Viral RNA Mini Kit (QIAGEN). The amount of viral RNA was determined by using primer binding in the 3′ nontranscribed region and the NP-coding region.

VP24. A definite reduction of VP24 in the lysates could be seen in cells transfected with the specific siRNAs directed against VP24 (Fig. 5A). The application of 250 ng (30 nM) of specific siRNAs was sufficient to silence VP24 (Fig. 5A, lanes 3 and 4). Probing the blots for the cellular protein α-tubulin revealed no detectable reduction of this constitutively expressed cellular protein (lanes 1 to 5). This indicated that the reduction of VP24 was not due to a general decrease in cellular proteins. The nonspecific siRNA X did not alter the amount of VP24, suggesting that the reduction of VP24 required siRNA molecules specifically targeted to the VP24 transcript sequences (Fig. 5A, lane 5).

Silencing of VP24 in MARV infection. Next, we investigated whether the siRNAs directed against VP24 could specifically reduce VP24 expression during MARV infection. We transfected each VP24-specific siRNA and the nonspecific siRNA X into Vero cells prior to infection. At 1 h postinfection, cells were transfected a second time with the same amounts of siRNAs. At 24 h postinfection, cells were harvested, and the amount of intracellular VP24 was monitored by Western blot analysis (Fig. 5B). A reduction of VP24 was seen for both siRNA sequences in MARV-infected cells (Fig. 5B, lanes 3 and 4) in comparison to cells left untreated (lane 2). Transfection of the nonspecific siRNA X had no effect on the expression level of VP24 (lane 5), indicating that the reduction of VP24 required specific targeting. Additionally, levels of the cellular proteins lamin A/C and α-tubulin were not changed, indicating that siRNA-induced silencing of VP24 during MARV infection is specific and not the result of a decrease in total protein production.

Ablation of VP24 has no effect on the intracellular levels of other viral proteins. Since we were able to accomplish VP24 silencing in infected cells, it was of interest to find out if downregulation of VP24 influenced the expression of other MARV proteins. To this end, Western blot analysis was performed with the cell lysates described above. As shown in Fig. 5B, silencing of VP24 did not lead to a significant decrease in levels of other viral proteins, suggesting that VP24 is not involved in transcription and replication. Moreover, these results showed that the mechanism of RNA interference is not able to degrade viral RNA genomes as this would result in a general decrease of viral proteins due to the loss of template. It is presumed that the genomic and antigenomic RNAs of nonsegmented negative-sense RNA viruses escape the onslaught of siRNA because they are tightly wrapped with the nucleoprotein NP, making them inaccessible to the double-stranded RNA and/or the RNA-induced silencing complex (3).

Ablation of VP24 leads to significant reduction of released infectious particles. It was further investigated whether VP24 silencing influenced the release of progeny virus. Therefore, MARV-infected cells were treated with VP24-specific siRNAs, and the amount of virus released into the culture medium was determined by Western blot analysis. NP was chosen as the target to monitor the amount of viral proteins in the supernatant since this protein is abundant in the virion and, in contrast to VP40, is not able to mediate its own release into the supernatant (data not shown). In non-siRNA-treated cells, MARV infection led to the release of viral particles at 24 h postinfection, as reflected by the appearance of NP in the supernatant (Fig. 5C, lane 2). Treatment of cells with siRNA not homologous to the MARV genome, siRNA X, had no effect on the release of NP from cells (Fig. 5C, lane 5). In contrast, the amount of released NP was significantly decreased when cells were treated with VP24-specific siRNAs (Fig. 5C, lanes 3 and 4). Real-time RT-PCR revealed that, as a result of VP24 silencing, the amount of genomic viral RNA present in the supernatant was also significantly reduced (Fig. 5D). The amplified fragment partly spanned the nontranscribed region of the 3′ end of the genome to make sure that only genomic RNA was addressed (24). These results were further supported by experiments monitoring infectious viral particles in the supernatant. Supernatants of siRNA-treated cells were harvested at 24 h postinfection and sequentially diluted. The dilutions were used to infect fresh Vero cells. At 8 days postinfection, cytopathic effect due to viral infection was monitored. Confirming the previous results, the amount of infectious particles was reduced by more than 95% compared with samples that were either treated with a nonspecific siRNA or only transfected with the transfection reagent (data not shown).

In summary, these experiments showed that VP24 was recruited into inclusions in MARV-infected cells by the presence of the major nucleocapsid protein NP. Additionally, VP24 was detected in single nucleocapsids outside the inclusions. VP24 was colocalized with VP40 at the plasma membrane, and recombinant expression revealed that VP24 was recruited into VP40-induced VLPs without altering the efficiency of budding. When the expression of VP24 in MARV-infected cells was downregulated by siRNA technology, the amount of released virus particles was significantly reduced.

DISCUSSION

VP24 was found to be colocalized with inclusions in MARV-infected cells that represent sites of formation and accumulation of nucleocapsids (21). Coexpression studies revealed that VP24 is recruited into the inclusions by the presence of NP. This is in line with results published by Huang and colleagues, who showed that formation of EBOV nucleocapsids could be accomplished only in the presence of VP24 (16). In contrast to the results of Huang and colleagues, we were not able to find evidence for a direct interaction between NP and VP24. A difference between our study and the one published by Huang et al. is that we used cell-based expression of NP and VP24 while Huang et al. used in vitro translation. It might be that a very weak interaction between NP and VP24 (suggested by the results of Huang et al.) was destroyed by cell lysis.

We present evidence that VP24 is connected to single nucleocapsids outside the inclusions, which are believed to be on the way from the inclusions to the plasma membrane. These data closely resemble results that we received for MARV VP40. VP40 was also detected in inclusions and with single nucleocapsids (20). Indeed, we were able to detect colocalization of VP24 and VP40 in viral inclusions (not shown). VP24 also showed a tendency to homooligomerize under physiological conditions. Preferentially tetrameric forms of the protein were detected. VP24 not only interacted with NP in the nucleocapsids but was also able to interact with cellular membranes. Interestingly, although the membrane interaction seemed to be weak or affected only a fraction of VP24 molecules, VP24 displayed features of an integral membrane pro-

tein. The membrane interaction of VP24 was not altered by the presence of other membrane-associated viral proteins like VP40 or GP. This indicated that the membrane interaction of VP24 is not mediated or influenced by other viral proteins. It is unclear whether homooligomeric forms of VP24 have a higher probability to bind to cellular membranes than the monomeric forms. Similar results have been presented for VP24 of the related EBOV (15). The characteristics of membrane binding of MARV VP24 resemble membrane binding of annexin V and XII that are partly soluble in the cytoplasm and can also bind to lipid membranes (17). Like the annexins, VP24 contains stretches of hydrophobic amino acids that might be suitable to interact with lipid membranes (not shown).

The ability of VP24 to bind to cellular membranes was confirmed by immunofluorescence and immunoelectron microscopic analyses. These experiments showed that VP24 was partly associated with the plasma membrane and partly with small unidentified intracellular vesicles. While VP24 was colocalized with VP40 at the plasma membrane of MARV-infected cells, intracellular membrane-associated VP24 was located separately from VP40. This holds true also for multivesicular bodies, which contained the highest intracellular concentrations of MARV VP40 and did not contain VP24 (20). The presence of GP, which is redistributed from the secretory pathway into peripheral multivesicular bodies by VP40 (19), also did not lead to the recruitment of VP24 into the peripheral multivesicular bodies.

It is believed that VP40 reaches the plasma membrane in two ways. On the one hand, VP40 is transported together with nucleocapsid; on the other hand, VP40 uses membranes of the late endosomes for its transport to the sites where budding takes place (18, 19). Data from the present study suggest that VP24 behaves in a similar way. The association with nucleocapsids suggests that VP24 is cotransported with these, while the interaction of VP24 with small lipid vesicles and its appearance at the plasma membrane upon single expression additionally point to a VP40- and nucleocapsid-independent transport pathway to reach the plasma membrane.

In contrast to VP24 of EBOV, VP24 of MARV did not display budding activity (15). The difference might be caused by the lack of a potential late domain motif in the sequence of MARV VP24 in contrast to EBOV VP24, which contains an YXXL motif (15). The presented data indicate that MARV VP24 is recruited into the released particles by the activity of VP40. Interestingly, VP24 was not recruited into VLPs that are induced by expression of GP. This suggested a specific targeting of VP24 to VP40-positive membrane compartments at the plasma membrane. The recruitment of VP24 into VP40-induced VLPs did not alter the efficiency of their release into the medium. This is consistent with the findings reported for the recruitment of EBOV VP24 into VLPs (22) and suggests that VP24 does not influence budding efficiency.

VP24 obviously does play an essential role in the replication cycle of MARV since the downregulation of VP24 in MARV-infected cells significantly impaired the release of progeny infectious virions. Based on the results that (i) silencing of VP24 did not impair transcription and replication, as demonstrated by the fact that the expression levels of the other viral proteins were not altered significantly and by a previous finding that VP24 did not influence transcription and replication in a MARV minigenome system (24); (ii) VP24 interacted with nucleocapsids, which represent the templates for the viral RNA-dependent RNA polymerase; and (iii) VP24 did not affect budding, the following hypothesis concerning the role of VP24 is suggested. VP24 is important for a step in the viral replication cycle after nucleocapsids have served as templates for replication and transcription and before the budding of progeny virions. This might be the assembly of transport-competent nucleocapsids, the association of nucleocapsids with the transport machinery (most likely the cytoskeleton), and/or the targeting of the nucleocapsids to the sites of budding where VP40 and GP are concentrated (19). Experiments to address these questions are under way.

A study by Watanabe et al. suggested that VP24 of EBOV is not essential for the release of infectious EBOV-specific VLPs which contain an artificial minigenome (31). The difference between this study and ours, in which VP24 was a crucial factor for the release of infectious MARV particles, might be caused by the fact that packaging of the artificial nucleocapsid encapsidating a minigenome which consisted only of approximately 1/10 of the wild-type genome is independent of VP24. The artificial nucleocapsid is presumed to be considerably smaller than the wild-type nucleocapsid (5). On the other hand, Watanabe et al. showed that, to a certain extent, VP24 influenced the efficiency of release of infectious VLPs (31). The effect was dependent on the amount of the plasmid encoding EBOV VP24. While large amounts of VP24 seemed to be inhibitory, small amounts enhanced the number of released infectious particles. It is not clear which of the transfected amounts of plasmids led to protein levels corresponding to infected cells. It is therefore an open question whether, under conditions that correspond to viral infection, VP24 of EBOV shows similar effects on the release of particles as described here for VP24 of MARV.

In summary, our study showed that VP24 of MARV is recruited to the viral inclusions and to single nucleocapsids outside the inclusions by NP, the major nucleocapsid protein. Additionally, VP24 was recruited into VP40-induced VLPs but did not alter the budding efficiency of VLPs containing either VP40 or VP40 and GP. Silencing of VP24 in MARV-infected cells showed that this protein plays a crucial role in the release of infectious progeny virions.

ACKNOWLEDGMENTS

The authors thank Angelika Lander, Inge Lettermann-Nass, and Sonja Heck for expert technical assistance.

This work was supported by the Deutsche Forschungsgemeinschaft, Sonderforschungsbereich 535 TP A13 and 593 TP B3, and by the Land Hessen through a fellowship to S. Bamberg.

REFERENCES

1. **Becker, S., C. Rinne, U. Hofsass, H. D. Klenk, and E. Mühlberger.** 1998. Interactions of Marburg virus nucleocapsid proteins. Virology **249:**406–417.
2. **Bergmann, J. E., and P. J. Fusco.** 1988. The M protein of vesicular stomatitis virus associates specifically with the basolateral membranes of polarized epithelial cells independently of the G protein. J. Cell Biol. **107:**1707–1715.
3. **Bitko, V., and S. Barik.** 2001. Phenotypic silencing of cytoplasmic genes using sequence-specific double-stranded short interfering RNA and its application in the reverse genetics of wild type negative-strand RNA viruses. BMC Microbiol. **1:**34.
4. **Bordier, C.** 1981. Phase separation of integral membrane proteins in Triton X-114 solution. J. Biol. Chem. **256:**1604–1607.
5. **Cheusova, T. B., S. Becker, E. Muehlberger, and E. I. Ryabchikova.** 2002. Submicroscopic characteristics of Marburg virus and its mini genome

analog replication in cell cultures. Mol. Gen. Mikrobiol. Virusol. **2:**27–30. (In Russian.)
6. **Elbashir, S. M., J. Harborth, W. Lendeckel, A. Yalcin, K. Weber, and T. Tuschl.** 2001. Duplexes of 21-nucleotide RNAs mediate RNA interference in cultured mammalian cells. Nature **411:**494–498.
7. **Feldmann, H., and M. P. Kiley.** 1999. Classification, structure, and replication of filoviruses. Curr. Top. Microbiol. Immunol. **235:**1–21.
8. **Feldmann, H., E. Muhlberger, A. Randolf, C. Will, M. P. Kiley, A. Sanchez, and H. D. Klenk.** 1992. Marburg virus, a filovirus: messenger RNAs, gene order, and regulatory elements of the replication cycle. Virus Res. **24:**1–19.
9. **Feldmann, H., C. Will, M. Schikore, W. Slenczka, and H. D. Klenk.** 1991. Glycosylation and oligomerization of the spike protein of Marburg virus. Virology **182:**353–356.
10. **Felgner, J. H., R. Kumar, C. N. Sridhar, C. J. Wheeler, Y. J. Tsai, R. Border, P. Ramsey, M. Martin, and P. L. Felgner.** 1994. Enhanced gene delivery and mechanism studies with a novel series of cationic lipid formulations. J. Biol. Chem. **269:**2550–2561.
11. **Fowler, T., S. Bamberg, P. Möller, H.-D. Klenk, T. F. Meyer, S. Becker, and T. Rudel.** 2005. Inhibition of Marburg virus protein expression and viral release by RNA interference. J. Gen. Virol. **86:**1181–1188.
12. **Fuerst, T. R., E. G. Niles, F. W. Studier, and B. Moss.** 1986. Eukaryotic transient-expression system based on recombinant vaccinia virus that synthesizes bacteriophage T7 RNA polymerase. Proc. Natl. Acad. Sci. USA **83:**8122–8126.
13. **Funke, C., S. Becker, H. Dartsch, H. D. Klenk, and E. Muhlberger.** 1995. Acylation of the Marburg virus glycoprotein. Virology **208:**289–297.
14. **Ge, Q., M. T. McManus, T. Nguyen, C. H. Shen, P. A. Sharp, H. N. Eisen, and J. Chen.** 2003. RNA interference of influenza virus production by directly targeting mRNA for degradation and indirectly inhibiting all viral RNA transcription. Proc. Natl. Acad. Sci. USA **100:**2718–2723.
15. **Han, Z., H. Boshra, J. O. Sunyer, S. H. Zwiers, J. Paragas, and R. N. Harty.** 2003. Biochemical and functional characterization of the Ebola virus VP24 protein: implications for a role in virus assembly and budding. J. Virol. **77:**1793–1800.
16. **Huang, Y., L. Xu, Y. Sun, and G. J. Nabel.** 2002. The assembly of Ebola virus nucleocapsid requires virion-associated proteins 35 and 24 and posttranslational modification of nucleoprotein. Mol. Cell **10:**307–316.
17. **Isas, J. M., J. P. Cartailler, Y. Sokolov, D. R. Patel, R. Langen, H. Luecke, J. E. Hall, and H. T. Haigler.** 2000. Annexins V and XII insert into bilayers at mildly acidic pH and form ion channels. Biochemistry **39:**3015–3022.
18. **Kolesnikova, L., S. Bamberg, B. Berghofer, and S. Becker.** 2004. The matrix protein of Marburg virus is transported to the plasma membrane along cellular membranes: exploiting the retrograde late endosomal pathway. J. Virol. **78:**2382–2393.
19. **Kolesnikova, L., B. Berghöfer, S. Bamberg, and S. Becker.** 2004. Multivesicular bodies as a platform for the formation of Marburg virus envelope. J. Virol. **78:**12277–12287.
20. **Kolesnikova, L., H. Bugany, H. D. Klenk, and S. Becker.** 2002. VP40, the matrix protein of Marburg virus, is associated with membranes of the late endosomal compartment. J. Virol. **76:**1825–1838.
21. **Kolesnikova, L., E. Mühlberger, E. Ryabchikova, and S. Becker.** 2000. Ultrastructural organization of recombinant Marburg virus nucleoprotein: comparison with Marburg virus inclusions. J. Virol. **74:**3899–3904.
22. **Licata, J. M., R. F. Johnson, Z. Han, and R. N. Harty.** 2004. Contribution of Ebola virus glycoprotein, nucleoprotein, and VP24 to budding of VP40 virus-like particles. J. Virol. **78:**7344–7351.
23. **Modrof, J., C. Moritz, L. Kolesnikova, T. Konakova, B. Hartlieb, A. Randolf, E. Mühlberger, and S. Becker.** 2001. Phosphorylation of Marburg virus VP30 at serines 40 and 42 is critical for its interaction with NP inclusions. Virology **287:**171–182.
24. **Mühlberger, E., B. Lotfering, H. D. Klenk, and S. Becker.** 1998. Three of the four nucleocapsid proteins of Marburg virus, NP, VP35, and L, are sufficient to mediate replication and transcription of Marburg virus-specific monocistronic minigenomes. J. Virol. **72:**8756–8764.
25. **Saksela, K.** 2003. Human viruses under attack by small inhibitory RNA. Trends Microbiol. **11:**345–347.
26. **Sänger, C., E. Muhlberger, E. Ryabchikova, L. Kolesnikova, H. D. Klenk, and S. Becker.** 2001. Sorting of Marburg virus surface protein and virus release take place at opposite surfaces of infected polarized epithelial cells. J. Virol. **75:**1274–1283.
27. **Sutter, G., M. Ohlmann, and V. Erfle.** 1995. Non-replicating vaccinia vector efficiently expresses bacteriophage T7 RNA polymerase. FEBS Lett. **371:**9–12.
28. **Swenson, D. L., K. L. Warfield, K. Kuehl, T. Larsen, M. C. Hevey, A. Schmaljohn, S. Bavari, and M. J. Aman.** 2004. Generation of Marburg virus-like particles by co-expression of glycoprotein and matrix protein. FEMS Immunol. Med. Microbiol. **40:**27–31.
29. **Traggiai, E., S. Becker, K. Subbarao, L. Kolesnikova, Y. Uematsu, M. R. Gismondo, B. R. Murphy, R. Rappuoli, and A. Lanzavecchia.** 2004. An efficient method to make human monoclonal antibodies from memory B cells: potent neutralization of SARS coronavirus. Nat. Med. **10:**871–875.
30. **Volchkov, V. E., A. A. Chepurnov, V. A. Volchkova, V. A. Ternovoj, and H. D. Klenk.** 2000. Molecular characterization of guinea pig-adapted variants of Ebola virus. Virology **277:**147–155.
31. **Watanabe, S., T. Watanabe, T. Noda, A. Takada, H. Feldmann, L. D. Jasenosky, and Y. Kawaoka.** 2004. Production of novel Ebola virus-like particles from cDNAs: an alternative to Ebola virus generation by reverse genetics. J. Virol. **78:**999–1005.